Damage characteristic of rock sample with circular defect based on the distinct element and moment tensor methods

Baowen Hu[1, 2], Changhong Li[2*]

[1]*School of Civil and Environmental Engineering, University of Science and Technology Beijing, Beijing, China*

[2]*State Key Laboratory of High-Efficient Mining and Safety of Metal Mines, Ministry of Education, Beijing, China*

Received 2 August 2014, www.cmnt.lv

Abstract

Based on the distinct element and moment tensor theory, the damage process and mechanism of rock sample with circular hole were researched. The crack evolution patterns corresponding to the laboratory test showed that there were mainly four stages. Firstly, the microcracks were randomly distributed in the rock sample. Secondly, the larger primary cracks are formed around top of circular hole with the increasing of microcracks. Then, more microcracks were localized near the boundary of circular hole, which formed the competition of several possible sets of fractures. Finally, the rupture zone was formed along one of crack zones. The size effect of circular hole showed that there would take on different rupture forms with increasing of diameter. Meanwhile, for better probing into damage mechanism, the acoustic emission (AE) algorithm based on moment tensor theory was implanted into the whole loading process. The AE magnitudes of all parts of rock sample were shown in AE contour maps, and these contour maps showed that the formations of rupture zone were contributed by different stress or energy levels.

*Keywords: c*ircular hole, damage mechanism, acoustic emission, distinct element, moment tensor

1 Introduction

There has been a substantial effort by engineers to probe into the damage and fracture propagation around underground excavations. It is generally thought that, for a circular opening in a brittle rock subjected to different stress fields, there mainly exist three types of fracture: spalling fracture caused by compressive stress field, primary fracture caused by tensile stress field, and remote fracture caused by mixture effect of compressive and tensile stress field [1-3]. For further understanding the damage process, various research methods were employed and developed. One approach often used is to build theoretical models and find analytical solutions. Sharan [4] finished the analytical solution for stress and displacement around a circular opening in a generalized Hoek-Brown rock. Zhang [5] obtained the stress and deformation solution of circular opening in strain-softening rock mass. In addition, the effect of seepage force was considered in the theoretical models [6, 7]. Although the analytical methods can facilitate us to understand the mechanical mechanism of deformation and failure characteristics from perspective of continuum mechanism, after all, some of results are lack of evidences from field and laboratory experiments [8], and cannot easily probe into the entire fracture process from meso-scale. Therefore, the physical test and numerical simulation methods are adopted by many researchers in recent years. However, some of simulation works focused on the loading type failure of Berea sandstone and didn't consider the size effect of circular hole [9, 10]. As we know, the lithology and size effect of circular hole would influence on the rupture characteristic. With respect to the simulation method, the distinct element method would be more practical in modelling the entire fracture process, which involves the initiation, propagation, and coalescence of micro-cracks through to the formation of a full-scale macro-crack in the rock materials [11], compared other methods like fast lagrangian analysis of continua or finite element method [10, 12]. Because mesh discretization is not necessarily considered in this way, namely the mesh sensitivity problem is not present.

For these reasons, take the previous laboratory experiment done by Lv [13] as reference, the aim of our work is to further reveal progressive failure leading to collapse around a circular opening in granite specimen by virtue of simulation of particle flow code (PFC2D). The opening size effect is considered. Meanwhile, for better understanding the damage process and mechanism, the acoustic emission (AE) algorithm based on the moment tensor theory is used in the simulation.

2 Laboratory experimental model

The rock samples used in the test were granite materials which were obtained from Dagangshan Hydropower Station in Sichuan Province of China. The uniaxial compression strength is 195MPa, the Young's modulus is 47.6GPa, the Poisson ratio is 0.23, and the tensile strength is 6.2MPa. To simulate the underground opening,

[*]***Corresponding author*** e-mail: lch@ustb.edu.cn

rectangular rock plates containing a 10mm diameter hole in centre were tested in servo-controlled hydraulic test machine (type: RMT-150C). The size of the rock plate was designed to 60 mm × 20 mm × 120 mm (length, width, height). Then the rectangular rock plates with a circular opening were loaded to failure under uniaxial compression test. Partial experimental results finished by Lv [13] are listed above. Figures 1a, 1b, 1c shows the failure process of rock plate, which represents the initiation of primary cracks, the expanding of remote cracks and compression-shear cracks, and the generation of rupture zone due to the coalescence of cracks respectively. Figure 2 shows the variation of compressive stress and AE events with axial strain.

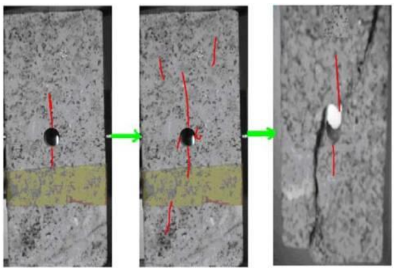

FIGURE 1 Failure process of rock samples

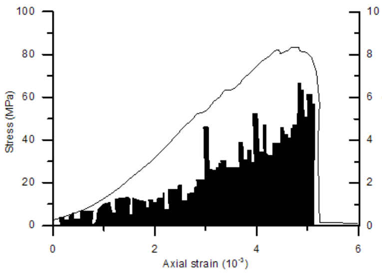

FIGURE 2 Compressive stress and AE event number versus axial strain

3 Establishment of numerical model and loading test

PFC2D is a distinct element computer program designed to simulate the mechanical behaviour of bonded or unbounded granular materials. Therefore the rock sample can be treated as assembly of circular particles that can interact through normal and shear springs. Although PFC2D can simulate a particulate media, any circular element in this program does not necessarily model a particle in the real material as two-dimensional nature of the program limits particles to disks or cylinders [9]. So we used this software as an attempt to mimic the basic mechanical features of actual material.

Before establish the numerical rock sample, numerical calibration test were necessary [14]. The micro-mechanical parameters were needed to be adjusted repeatedly, and finalized until the macroscopic properties such as Young's modulus and the uniaxial compressive strength calculated are basically consistent with physical macroscopic parameters.

The micro-parameters required to be adjusted are as follows: ρ is ball density, $R_{\min}$ is minimum ball radius, R_ratio is ball size ratio, $\bar{\lambda}$ is parallel-bond radius multiplier, E_c is ball-ball contact modulus, $\overline{E_c}$ is parallel-bond modulus, k_n / k_s is ball stiffness ratio, $\bar{k}_n / \bar{k}_s$ is parallel bond stiffness ratio, μ is ball friction coefficient, $\bar{\sigma}_c$ is parallel bond normal strength, and $\bar{\tau}_c$ is parallel-bond shear strength. The values of micro-parameters are listed in Table 1.

TABLE 1 Micro-mechanical parameters of numerical samples

$\rho/(kg.m-3)$	$R_{\min}$ / (mm)	R_ratio	μ	
2500	0.3	2.0	0.5	
$\bar{\sigma}_{mean}$ / (MPa)	$\bar{\tau}_{mean}$ / (MPa)	$\bar{\sigma}_{sdev}$ / (MPa)	$\bar{\tau}_{sdev}$ / (MPa)	
100	100	36	36	
k_n / k_s	$\bar{k}_n / \bar{k}_s$	E_c / (GPa)	$\overline{E_c}$ / (GPa)	$\bar{\lambda}$
2.5	2.5	37.6	37.6	1.0

There are mainly four steps for the creation of corresponding rock samples according to the micromechanics parameters that have been determined by calibration tests. Firstly, a rectangular specimen consisting of arbitrarily placed particles confined by four frictionless walls is generated by radius expansion method. Secondly, radii of all particles are changed uniformly to achieve a specified isotropic stress so as to reduce the magnitude of locked-in stresses that will develop after subsequent bond-installation and specimen-unloading steps. In this paper the isotropic stress is set to 0.1MPa. Thirdly, the floating particles that have less than three contacts are eliminated. Fourthly, the parallel bonds are installed throughout the assembly between all particles that are in near proximity to finalize the specimen.

As the generation of rock sample was completed, then circular holes with diameter from 10mm to 50mm were excavated respectively since the size effect of circular hole on failure characteristic of rock sample would be researched. In addition, the AE algorithm was implanted into the whole failure process for recording the AE event and magnitude.

4 Acoustic emission algorithm based on moment tensor theory

There are essentially two ways that have been adopted to extract seismic or AE information from bond breakages in PFC [15-17]. Initially, the magnitude of AE events from the kinetic energy of the particles in each crack was calculated, and moment tensor was also calculated from the force at the contact as breakage of bond occurs. However, this method often yields magnitudes that are too large. Besides, it fails to account for shear events where the entire force at the contact is not lost. For solving the problem, the moment tensor of AE events was recalculated by observing the force changes at contacts around the source particles, and moment magnitudes were then calculated form the moment tensor matrix. Therefore the second computing method was used in this paper to further probe into the damage mechanisms of rock samples with circular hole.

The Equation for calculating a moment tensor for an AE event is as following:

$$M_{ij} = \sum_{S} \Delta F_i R_j \, , \tag{1}$$

where ΔF_i is i-th component of the change in contact force, and R_j is j-th component of the distance between the contact point and event centroid. The centroid of the event is assumed to be the geometric centre of multiple-crack events since each AE event could be composed of more than one bond breakage. The sum is performed over source boundary which is a surface that completely encloses the displacement discontinuity caused by the 'fault'. As we know the moment tensor is a function of time because it will be calculated at each time step over the duration of the event. The duration of AE event is determined by assuming a fracture propagates at half the shear wave velocity of the rock. Therefore, for reducing memory consumption, the final moment tensor that is independent of time is determined to be the moment tensor at the time of maximum scalar moment. The formulation of the scalar moment is as following:

$$M_0 = \left(\frac{\sum_{j=1}^{3} m_j^2}{2} \right)^{1/2} , \tag{2}$$

where m_j are the eigenvalues of the moment tensor matrix. By virtue of the scalar moment, the moment magnitude of the event can be calculated by this following Equation:

$$M_w = \frac{2}{3} \log M_0 - 6 \tag{3}$$

5 Numerical experiment results and discussion

5.1 CRACK EVOLUTION AND AE CHARACTERISTIC

Figure 3 shows the numerically simulated failure process around a circular opening with diameter 10 mm. The black and red spots represent the bond breakage as the result of its normal and shear strength being exceed respectively. Each green circle represents an AE event, and its radius represents the range of AE event, i.e. one AE event may contain many bond breakages. At the beginning loading stage (Figure 3a), there are some independent microcracks (bond breakages) distributed randomly in the rock sample, which lead to the production of AE events. In this period, most of AE events consist of a series of single microcrack event, only few are made up of more than one microcrack events. In the second stage (Figure 3b, axial strain is about 1e-3), it can be observed that more microcracks are generated in the rock sample, and the larger primary cracks are formed around top of circular hole. As the axial strain is getting to around 1.5e-3 (Figure 4), more microcracks localize near the lateral boundaries of the circular opening and begin to form rupture zones on both sides of specimen (Figure 3c). Meanwhile, the remote cracks are produced and expanded. The number of AE events starts to increase, and the radius of some green circles have become larger, which means the larger scale cracks form, and magnitudes of partial AE events also become increasingly. Finally, as the axial strain gets to around 2e-3, the rock sample shows a macroscopic discontinuity along the rupture zone (Figure 3d), and the number of AE events gets to the maximum nearby the peak of loading stress (Figure 4).

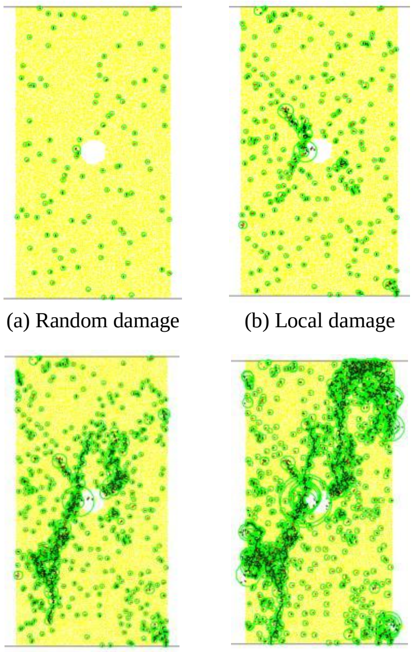

(a) Random damage (b) Local damage

(c) Damage expanding (d) Rupture zone

FIGURE 3 Simulated failure process of rock sample

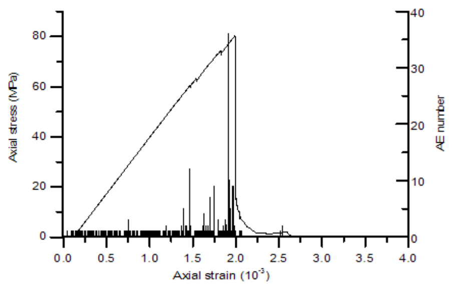

FIGURE 4 Simulated compressive stress and AE event number versus axial strain

The Figure 5 demonstrates the contour map of moment magnitude of AE event, which is corresponding to the Figure 3d. As we can see, the magnitudes of main rupture zone represented by red colour are between -4.9 and -4.7 which means such kind of magnitude can fully satisfy the generation of rupture zone developed by the coalescence of the microcracks. Outsides of main rupture zone, the magnitudes are mainly between -5.5 and -5, which means these smaller scale damages fail to connect each other to produce the larger scale cracks. In short, such kind of simulation based on the distinct element and moment tensor theory can better reveal and demonstrate the damage process and mechanism of rock sample. The results of magnitude calculated by scalar moment match very well with simulated damage distribution and actual lab test.

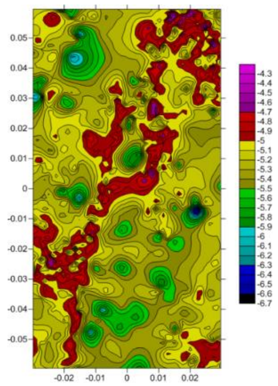

FIGURE 5 Contour map of magnitude of AE event

Although the simulated curve of compressive stress versus the axial strain shows a slightly stiffer response, the whole variation trend and peak value are basically in agreement with the actual laboratory test. As for number of AE events versus axial strain, the variation trend also has similarity with actual lab test despite of concrete number of AE event, because we only care about basic mechanical features and laws.

5.2 THE SIZE EFFECT OF CIRCULAR HOLE

The influences of different sizes of circular hole on the final rupture zones of the rock sample are considered in this section. As the diameters are between 10 mm and 30 mm (Figure 3d, Figures 6a-6b), there are longitudinal crack zones generated nearby the top or bottom of the circular hole, especially for the diameter 30 mm, because the increment of size of circular hole reduces the tensile strength on the periphery of hole, and the values of tensile stress on the top and bottom of hole are also larger than other direction. However, more microcracks localize near the lateral boundaries of the circular hole and form notches, and finally the failure plane extends from the notches in the inclined direction; As the diameters are greater than 40mm, the rock sample shows the symmetrical failure along the rupture zone of which the direction is sub-horizontal.

It is interesting to note that the maps of contour of magnitude of AE event, there still take on red colour in the core area of rupture zones. However, periphery of red colour is mainly encompassed by the yellow colour, part of which is still in the rupture zone, and of which the magnitudes are lower than red colour. Such kind of phenomenon is more obvious as the diameter of circular hole is greater than 20 mm. There are mainly two reasons we think lead to this kind of phenomenon.

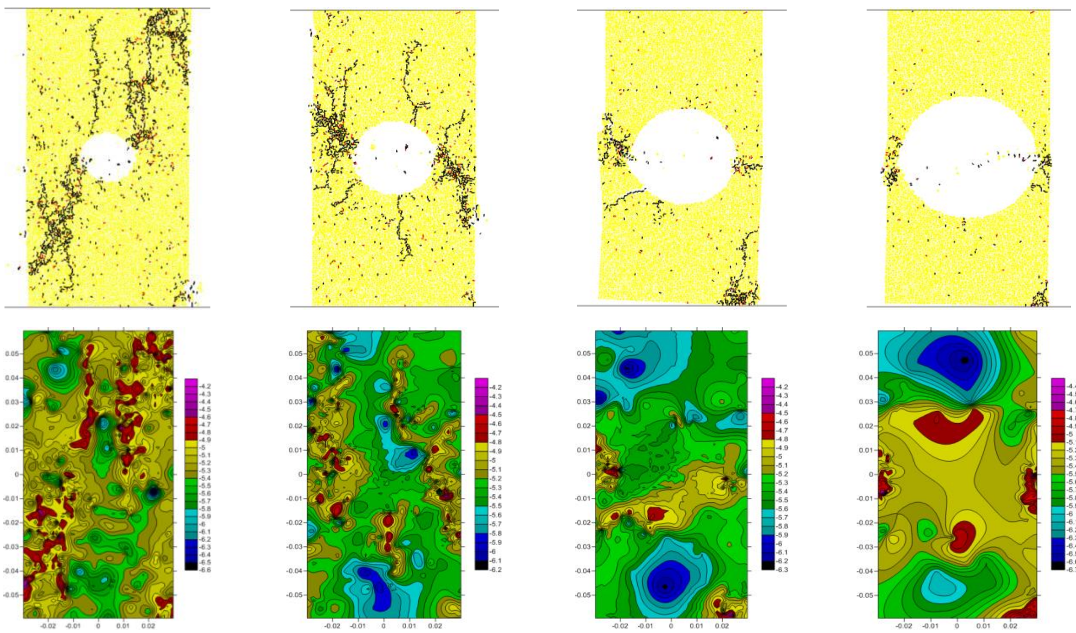

a b c d

FIGURE 6 Crack patterns of rock sample and contour maps of magnitude of AE event and under different diameters of circular hole including 20 mm, 30 mm, 40 mm, 50 mm

It is interesting to note that the maps of contour of magnitude of AE event, there still take on red colour in the core area of rupture zones. However, periphery of red colour is mainly encompassed by the yellow colour, part of which is still in the rupture zone, and of which the magnitudes are lower than red colour. Such kind of phenomenon is more obvious as the diameter of circular hole is greater than 20 mm. There are mainly two reasons we think lead to this kind of phenomenon. On the one hand, the different stress or energy levels can come together to promote propagation of the rupture zone. Some core ruptures are mainly finished by the higher magnitude of stress or energy then the lower stress or energy finishes extension and coalescence of the rupture zone on the basis of core rupture zone. On the other hand, the increasing of size of circular hole equivalently increases the damage degree of rock sample and decreases the compressive strength as we can see from the Figure 7, which make the relatively lower stress or energy easier to generate the cracks.

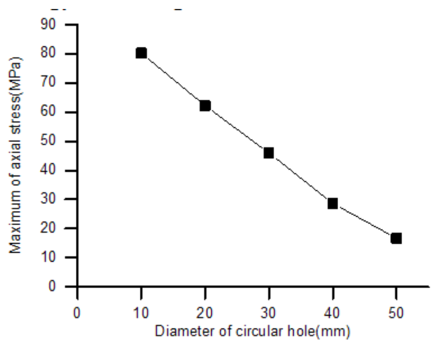

FIGURE 7 the maximum of axial stress versus the diameter of circular hole

6 Conclusions

In this study, the failure process of granite sample with circular hole was simulated by the distinct element method. The numerically simulated results reproduced the development of cracks around a circular opening in rock, which were in very agreement with the laboratory test and also can reveal microscopic damage characteristic. The microcrack pattern showed that competition of several possible sets of fractures, eventually the cracks on both sides of circular hole prevailed and continued to propagate until the final rupture zone was formed. The simulated number of AE events would get peak as failure occurred, which was consistent with actual test.

The AE algorithm based on the moment tensor theory was used in the simulation, which can better reveal the damage mechanism for the loading test. Especially, the AE magnitude contour map can tell us intuitively the damage degree in different parts of rock sample.

The size effect of circular hole was considered in this paper. It showed that the crack development and distribution were influenced by the size of diameter, because the size of circular hole determines the prefabricated damage degree of the rock sample. In addition the contour map of AE magnitude showed that the formation of rupture zone were contributed by different stress or energy levels, and it would be more obvious with increasing of size of circular hole.

Acknowledgments

The authors are grateful for the financial support from the National Basic Research Program of China (973 Program) (2010CB731500). The authors also thank the professor Hazzard J.F. for providing the help about AE algorithm

References

[1] Martin C D 1997 The effect of cohesion loss and stress path on brittle rock strength *Canadian Geotechnical Journal* **34**(5) 159–68
[2] Napier J A L, Hildyard M W 1992 Simulation of fracture growth around openings in highly stressed brittle rock *Journal of the South African Institute of Mining and Metallurgy* **92**(6) 149-58
[3] Hoke E, Brown E T 1980 Underground excavation in rock *Metallurgical Industry London*
[4] Sharan S K 2008 Analytical solutions for stresses and displacements around a circular opening in a generalized Hoek-Brown rock *International Journal of Rock Mechanics and Mining Sciences* **45**(1) 78-85
[5] Zhang Q, Jiang B S, Wang S l, Ge X R 2012 Elasto-plastic analysis of a circular opening in strain-softening rock mass *International Journal of Rock Mechanics and Mining Sciences* **50**(2) 38-46
[6] Zareifard M R, Fahimifar 2014 A Effect of seepage forces on circular openings excavated in Hoek-Brown rock mass based on a generalised effective stress principle *European Journal of Environmental and Civil Engineering* **18**(5) 584-600
[7] Yang X L, Huang F 2010 Influences of strain softening and seepage on elastic and plastic solutions of circular openings in nonlinear rock masses *Journal of Central South University of Technology* **17**(3) 621-7
[8] Wang S, Hagan P, Cheng Y 2013 Experimental research on the instability characteristics of double-layer rock plates based on MTS-AE system *Applied Mathematics & Information Sciences* **7**(1L) 339-45
[9] Fakhimi A, Carvalho F, Ishida T 2002 Simulation of failure around a circular opening in rock *International Journal of Rock Mechanics and Mining Sciences* **39**(4) 507-15
[10] Wang S Y, Sloan S W, Sheng D C 2012 Numerical analysis of the failure process around a circular opening in rock *Computers and Geotechnics* **39**(1) 8-16
[11] Potyondy D, Cundall P, 2001 The PFC model for rock: predicting rock-mass damage at the underground research laboratory *Itasca Consulting Group*, Inc. Report no. 06819-REP-01200-10061-R00
[12] Li D, Li X, Li C C 2010 Experimental and numerical studies of mechanical response of plate-shape granite samples containing prefabricated holes under uniaxial compression *Chinese Journal of Rock Mechanics and Engineering* **30**(6) 1198-206 (*in Chinese*)
[13] Lv S, Chen W, Jia S, Tan X J 2009 Experimental study on brittle rock failure *Chinese Journal of Rock Mechanics and Engineering* **28** (SUPPL1) 2772-7
[14] Wang S R, Hagan P, Hu B W, Gamage K, Cheng Y, Xu D 2014 Rock-arch instability characteristics of the sandstone plate under different loading conditions *Advances in Materials Science and Engineering* Article ID 950870 1-9
[15] Hazzard J F, Young R P 2000 Simulating acoustic emissions in bonded-particle models of rock *International Journal of Rock Mechanics and Mining Sciences* **37**(5) 867–72
[16] Hazzard J F, Young R P 2002 Moment tensors and micromechanical models *Tectonophysics* **356**(1) 181–97 (*in Chinese*)
[17] Hazzard J F, Young R P 2004 Dynamic modelling of induced seismicity *International Journal of Rock Mechanics and Mining Sciences* **41**(8) 1365-76

Authors

Baowen Hu, born in May, 1984, Beijing, China

Current position, grades: the doctoral student of School of Civil and Environmental Engineering, University of Science and Technology Beijing, China.
University studies: M.Sc in Ecology from Chinese Academy of Sciences.
Scientific interest: mathematical model and numerical simulation of rock mechanics.
Publications: 10 papers.
Experience: 3 scientific research projects.

Changhong Li, born in October, 1962, Beijing, China

Current position, grades: the professor of School of Civil and Environmental Engineering, University of Science and Technology Beijing, China.
University studies: PhD in in Mining Engineering from University of Science and Technology Beijing.
Scientific interest: rock mechanics
Publications: 40 papers.